

BL37XU

Trace Element Analysis

1. Introduction

BL37XU is a hard X-ray undulator beamline for trace element analysis and chemical/elemental imaging dedicated to various X-ray spectroscopy methods such as scanning X-ray micro-spectroscopy, full-field X-ray micro-spectroscopy, and ultra-trace-element analysis [1]. Using these methods, research is actively conducted to elucidate the properties and functions of materials through analyses of the morphology, element distribution, chemical state, and local structure. In FY2022, BL37XU operated smoothly and almost all users completed their user time as scheduled. In addition, the following two projects were undertaken. (1) A new detector was installed for full-field imaging-type X-ray micro-spectroscopy. (2) A new vacuum chamber was constructed for scanning X-ray micro-spectroscopy.

2. Upgrade of the 2D detector for full-field imaging-type X-ray micro-spectroscopy

The computed tomography(CT) - X-ray Absorption Fine Structure -(XAFS) technique, which is a combination of X-ray CT and XAFS, is often used in full-field micro-spectroscopy. The exposure time of one projection image is about 10 ms in the projection-type method, whereas it is as long as several 100 ms to 1 s in the imaging-type method. Therefore, we updated the detector to reduce the measurement time of the imaging-type method.

We previously used a lens-coupled (LC) detector that is a combination of an X-ray visible-light-converted beam monitor (Hamamatsu Photonics, AA60) and an sCMOS camera

(Hamamatsu Photonics, ORCA-Flash 4.0 v2). In the LC type, X-rays are converted to visible light through a scintillator (P43, thickness: 10 μm) and led to the sCMOS sensor through a relay lens. The newly introduced X-ray sCMOS camera (Hamamatsu Photonics, C12849SPL) uses a fiber optic plate (FOP) to lead visible light to the sCMOS sensor with a very high transmission efficiency compared with the LC type.

The average intensity of the I_0 image at an incident X-ray energy of 7.7 keV was 25,640 counts/pixel/s in the LC type and 366,850 counts/pixel/s in the FOP type. The conversion factor from charge to counts of the sCMOS sensor was equal in the two detectors, but the intensity was 14 times higher in the FOP type. Figure 1 shows the mean squared error (MSE) of one-shot images at each exposure time based on the projection image with a long exposure time. Compared with the LC type, equivalent MSE images were obtained at 1/6 the exposure time in the FOP type. Figure 2 shows the X-ray chart pattern image (Applied Nanotools, HCAL-25nm). The exposure time required to see 100 nm L&S clearly was 800 ms–1 s for the LC type, while it was 100–150 ms for the FOP type. We

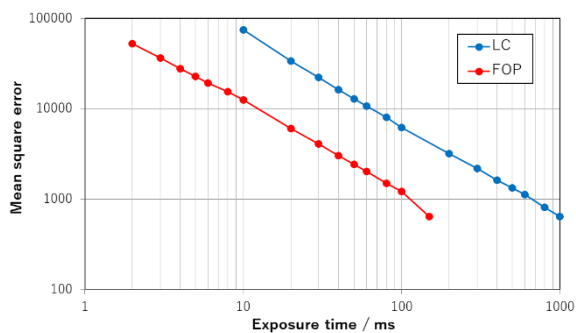


Fig. 1. Relationship of exposure time and mean square error.

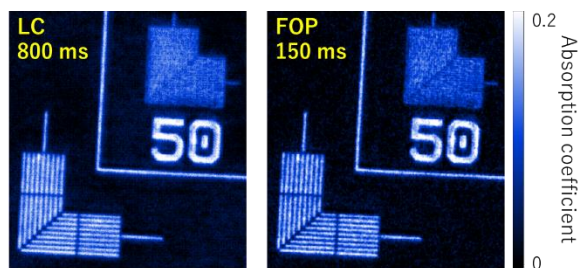


Fig. 2. X-ray chart pattern. Each upper-right pattern has 50 nm L&S, and the lower left pattern has 100 nm L&S.

successfully reduced the measurement time to about 1/10 of the time previously required for the imaging-type measurement.

3. Development of the vacuum chamber for scanning X-ray micro-spectroscopy

In scanning X-ray micro-spectroscopy, XAFS and XRF measurements have been performed using a 100 nm focused beam. It has been difficult to perform XRF measurements of elements lighter than K owing to absorption by air and interference from the overlapping fluorescence X-ray of argon, because the measurement environment is open to the atmosphere.

Therefore, we developed a vacuum chamber for hard X-ray 100 nm XRF measurement of those light elements. The seven-element silicon drift detector^[1] is available, but elements lighter than Na cannot be measured with the Be window material (25 μm). The sample stage is a 1 nm feedback stage (Sigma Koki, FS-1020UPX(V)) for vacuum use, which enables on-the-fly measurement synchronized with the stage encoder, and it is also equipped with a visible light microscope for observing sample positions.

As an example, we measured a piece of rock from a Yamato mercury mine. Figure 3 shows the visible light microscopy image, and the 2D XRF

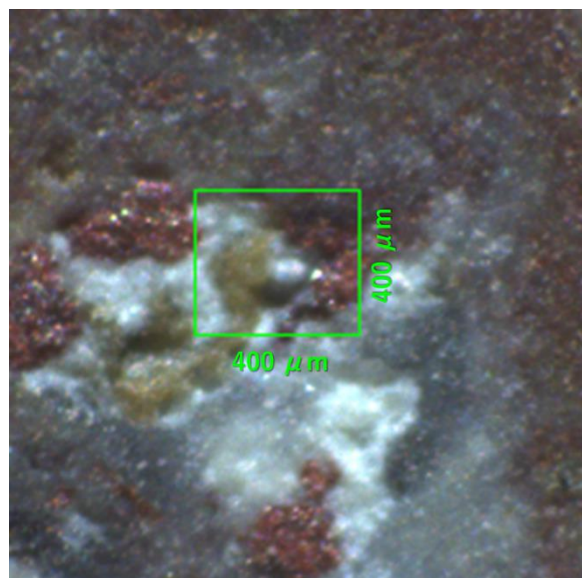


Fig. 3. Microscopy image of the sample.

measurement was performed on the area framed in green. Figure 4 shows the total XRF spectrum of the measurement area, and it was found that fluorescence X-rays of light elements such as Al, Si, S, and K, which are difficult to measure under atmospheric conditions, are well detected. Figure 5 shows the 2D XRF measurement results. The six images on the left show individual element maps, and the two images on the right show the elements overlaid with RGB. From the comparison of Fig. 3 and Fig. 5, it can be seen that the areas that appear vermilion in visible light are distributed with Hg and S, indicating that they are areas of cinnabar (HgS). Hard X-ray XRF imaging measurements are now available, including those of light elements, by using the vacuum chamber.

Nitta Kiyofumi and Sekizawa Oki

Spectroscopy Division, Center for Synchrotron Radiation Research, JASRI

Reference:

[1] Nitta, K. Sekizawa, O. & Suga, H. (2022). *SPring-8/SACLA Annual Report FY2021*, 65–67.

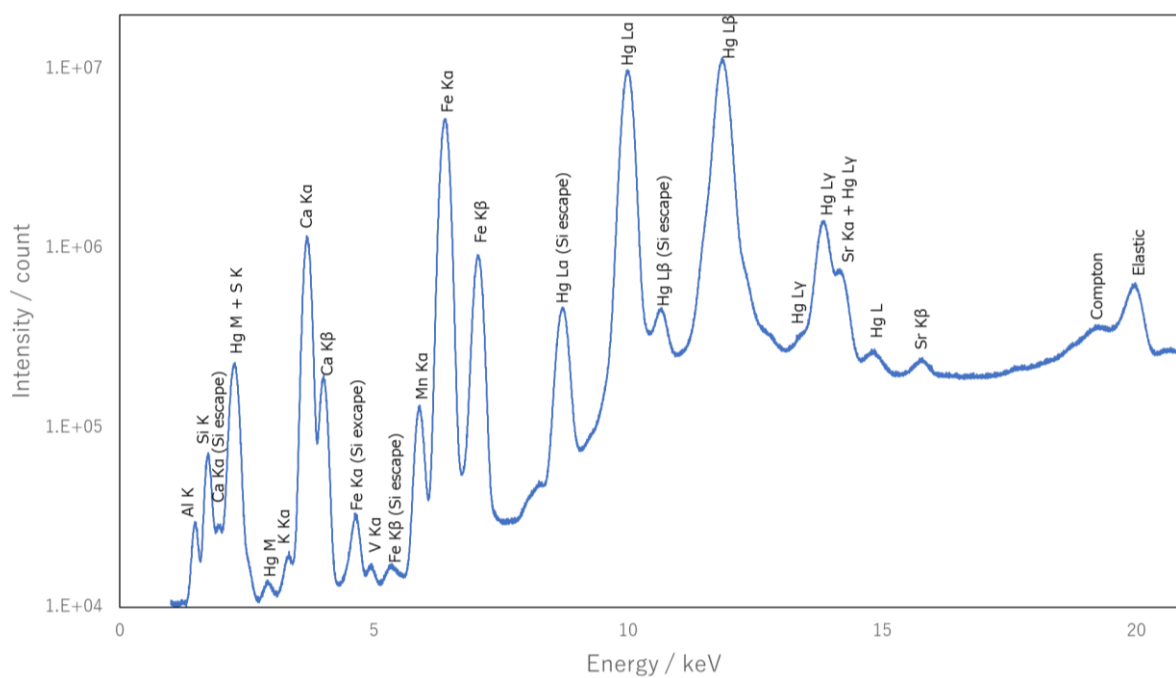


Fig. 4. Total XRF spectrum of the measurement area.

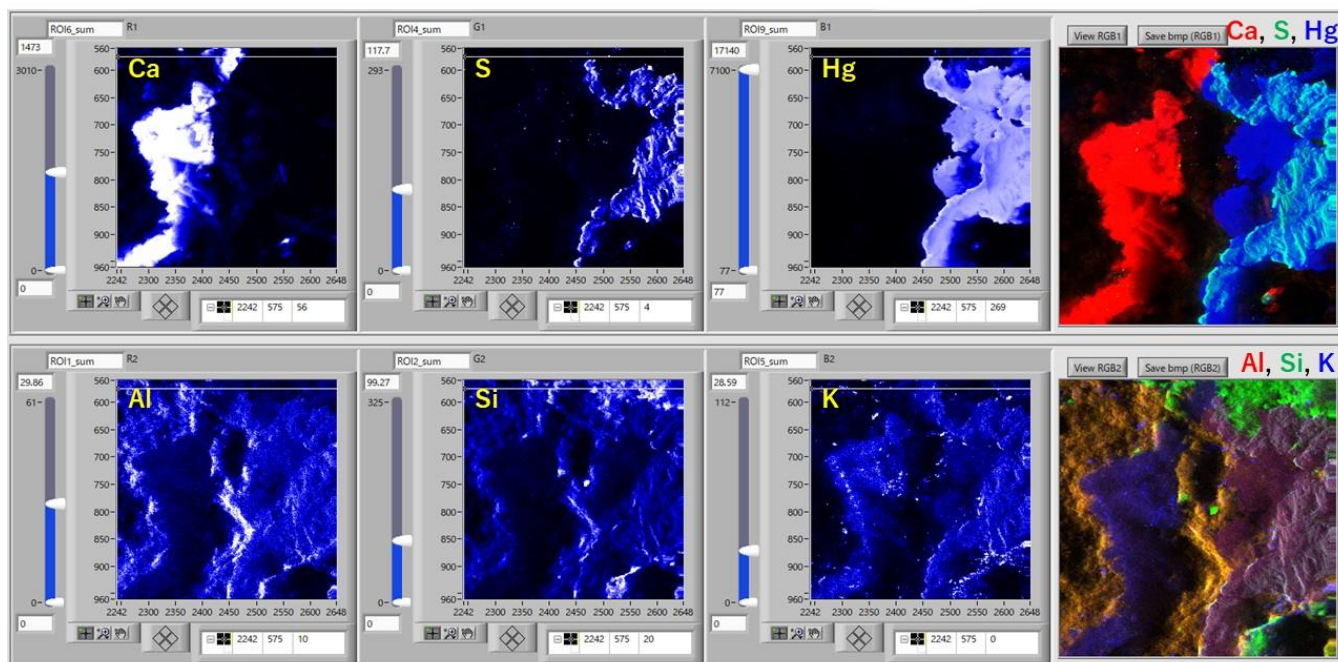


Fig. 5. Elemental maps of 2D XRF measurement. Incident X-ray energy: 20 keV, beam size: 200×200 nm, scan area: 400×400 μm, scan step: 1 μm, exposure time: 20 ms/point.